*J. Earth Syst. Sci.* (2020)129 124
https://doi.org/10.1007/s12040-020-01393-1
© Indian Academy of Sciences

# Dynamic recrystallization mechanisms and vorticity estimation of the Terrane Boundary Shear Zone (Lakhna shear zone): Implications on dynamics of juxtaposition of the Eastern Ghats Mobile Belt with the Bastar Craton, NW Odisha

Bhupesh Meher[1], Bhuban Mohan Behera[2,*] and Tapas Kumar Biswal[2]

[1]*Department of Geology, Central University of Kerala, Kerala 671 316, India.*
[2]*Department of Earth Sciences, Indian Institute of Technology Bombay, Mumbai 400 076, India.*
**Corresponding author. e-mail: beherabhubanmohan@gmail.com*

MS received 9 April 2019; revised 12 February 2020; accepted 16 February 2020

The Terrane Boundary Shear Zones provide important information regarding tectonics of juxtaposition between different terranes. In this paper, we have studied the Lakhna shear zone, between the Eastern Ghats Mobile Belt and the Bastar Craton. Detailed structural study, sampling and strain analysis through measurement of size and orientation of dynamically recrystallized quartz grains indicate: (i) the Lakhna shear zone is developed on granitic protolith of the Bastar Craton, (ii) mylonites are quartzofeldspathic in composition, marked by SE dipping mylonitic foliation and down dip stretching lineation defined by biotite and quartz grains, (iii) S-C fabric and rotated porphyroclasts indicate a NW vergence thrust kinematics, (iv) recrystallization of quartz grains occurred by climb-assisted dislocation creep through BLG near craton boundary, SGR in the central part of the shear zone, GBM towards the Eastern Ghats margin, (v) temperature of deformation increases towards mobile belt (380–560°C) that suggests thrusting of granulitic hot slab over cold craton and (vi) $W_m$ estimates of 0.9 suggest simple shear deformation. The juxtaposition between the EGMB and the Bastar Craton occurred by simple shear thrusting when the granulitic slab was hot enough to create a difference in temperature and mechanism of dynamic recrystallization across the shear zone.

**Keywords.** Lakhna shear zone; Eastern Ghats Mobile Belt; Bastar Craton; vorticity; differential stress.

## 1. Introduction

Peninsular India is marked by several prominent shear zones that define the terrane margin between craton and mobile belts. Study of such shear zones provides important information regarding the nature of juxtaposition between adjoining terranes. Shear zones are marked by differently oriented stretching lineation as per the sense of shear. The shear zones undergo general shear comprising a component of simple shear and pure shear component (Ramsay and Huber 1983, 1987; Passchier and Urai 1988; Wallis 1992, 1995; Wallis *et al.* 1993; Fossen and Tikoff 1993; Simpson and de Paor 1993). Vorticity of strain is generally nonuniform (Xypolias and Kokkalas 2006). Further, nature of dynamic recrystallization differs as a result of temperature and water content across the shear zone (Stipp *et al.* 2002). Grain size evolution during mylonitisation is controlled by the nature of creep

Published online: 20 May 2020

which depends on differential stress and strain rate (Platt and Behr 2011). Estimation of strain, temperature of deformation and differential stress help in understanding the dynamics of shearing. In our study, we have taken the Lakhna shear zone which is a part of the Terrane Boundary Shear Zone (TBSZ) between the Eastern Ghats Mobile Belt and the Bastar Craton in the NW part of Odisha, India.

A lot of researches have been carried out on this TBSZ to explain the shear kinematics and fold-thrust belt structure (Biswal 2000; Biswal *et al.* 2000, 2002); geochronological study from nepheline syenites (Biswal *et al.* 2004); petrofabric analysis of magmatic and tectonic fabric (Biswal *et al.* 2004) and global correlation with the Antarctica (Biswal *et al.* 2002), but there is very little study on the deformation mechanism based on dynamic recrystallization of the minerals (Biswal and Sinha 2003; Sinha *et al.* 2010). We have analyzed the process of dynamic recrystallization of quartz grain and strain distribution in quartzofeldspathic mylonite across the shear zone. This study will help to bridge the gap between micro-deformation analysis in the grain scale and large scale deformation in the field which would throw some light to understand the tectonothermal evolution of the shear zone and dynamics of the juxtaposition of the EGMB with the Bastar Craton. We have followed the geological map of Biswal *et al.* (2000) and plotted structural data and sample locations.

## 2. Geological setting

The Terrane Boundary Shear Zone (TBSZ) defines the tectonic line of the juxtaposition between the EGMB and the Dharwar–Bastar–Singhbhum cratons (figure 1). Many authors have described the tectonic boundary as Eastern Ghats boundary fault in the west and northwest (Ramakrishnan *et al.* 1998), Eastern Ghats Frontal Thrust in the southwest (Neogi and Das 1998), a part of charnockite line (Fermor 1936) and alkaline line (Leelanandam 1993). The TBSZ delineates a contrasting temporal and spatial variation of deformation style, lithological units and geochronology between the EGMB and the cratons. The craton consists of widespread occurrence of tonalite–trondhjemite–granodiorite gneisses (TTG, ca. 3500 Ma) that have been intruded by large scale potassic granite plutons (ca. 2500 Ma) (Ratre *et al.* 2010). Greenstone belts occur within TTG at several places, namely the Sonakhan Belts. The Bastar Craton is intruded by several dykes, varying in composition from basalt, dolerite, boninite, rhyolite to trachyte with an age of ca. 1.9–1.4 Ga (Crookshank 1963; Nanda *et al.* 1998; Gupta *et al.* 2000; Ratre *et al.* 2010). Majority of the dykes are unmetamorphosed, except for a few which show greenschist facies assemblages with relict igneous textures. Circumscribing the EGMB front, a number of sedimentary basins have been developed over the craton, hosting a Proterozoic platform sequence of rocks; these are known as the Purana basins (figure 1). The Khariar basin is one of those basins which are dominated by sandstone and shale sequence, while other basins like Chhattisgarh and Cuddapah, contain carbonates. The EGMB is dominated by granulite facies rocks namely khondalite, charnockite and mafic granulite (Grew and Manton 1986; Lal *et al.* 1987) and intrusives like anorthosite, gabbro, nepheline syenite (Biswal *et al.* 2004) and norite (Leelanandam 1990, 1993). The lithological assemblage of the EGMB was classified into five longitudinal zones, namely, western transition zone, western charnockite zone, western khondalite zone, central migmatites zone and eastern khondalite zone (Nanda and Pati 1989; Ramakrishnan 1990; Ramakrishnan *et al.* 1998) (figure 1). The TTG of the Bastar Craton indicates an age of ca. 3.5 Ga and the potassic granites as ca. 2.5 Ga (U–Pb zircon age, Sarkar *et al.* 1993). Dolerite, trachyte and rhyolite dykes in the Bastar Craton near Lakhna have been dated to be ca. 1.4 Ga (Ratre *et al.* 2010). The Bastar Craton is unconformably overlain by Khariar group of platform rocks which show a depositional age between ca. 1.4 and 0.5 Ga (Ratre *et al.* 2010). The EGMB was a tectonically inactive terrane during Archean and was marked by dynamothermal events belonging to Grenville and Pan-African ages. Time of juxtaposition of the EGMB against the Bastar Craton is inferred from alkali granite emplacement at ca. 1.5 Ga (Sarkar and Paul 1998; Aftalion *et al.* 2000) and ca. 0.5 Ga from nepheline syenite plutons (Biswal *et al.* 2007). The fission track dating of the mylonite samples indicates a slow cooling history marked by erosion and denudation of the area from $340 \pm 46$ to $268 \pm 34$ Ma and a local high temperature at 120 Ma has resulted during the passing of Indian plate over the Kerguelen hot spot (Biswal and Seward 2003).

Our study area belongs to the NW part of the TBSZ which is designated as the Lakhna shear zone (Biswal *et al.* 2002). The EGMB and the Bastar Craton form the hanging wall and footwall of the southeasterly dipping Lakhna shear zone (thrust). The western transition zone and western

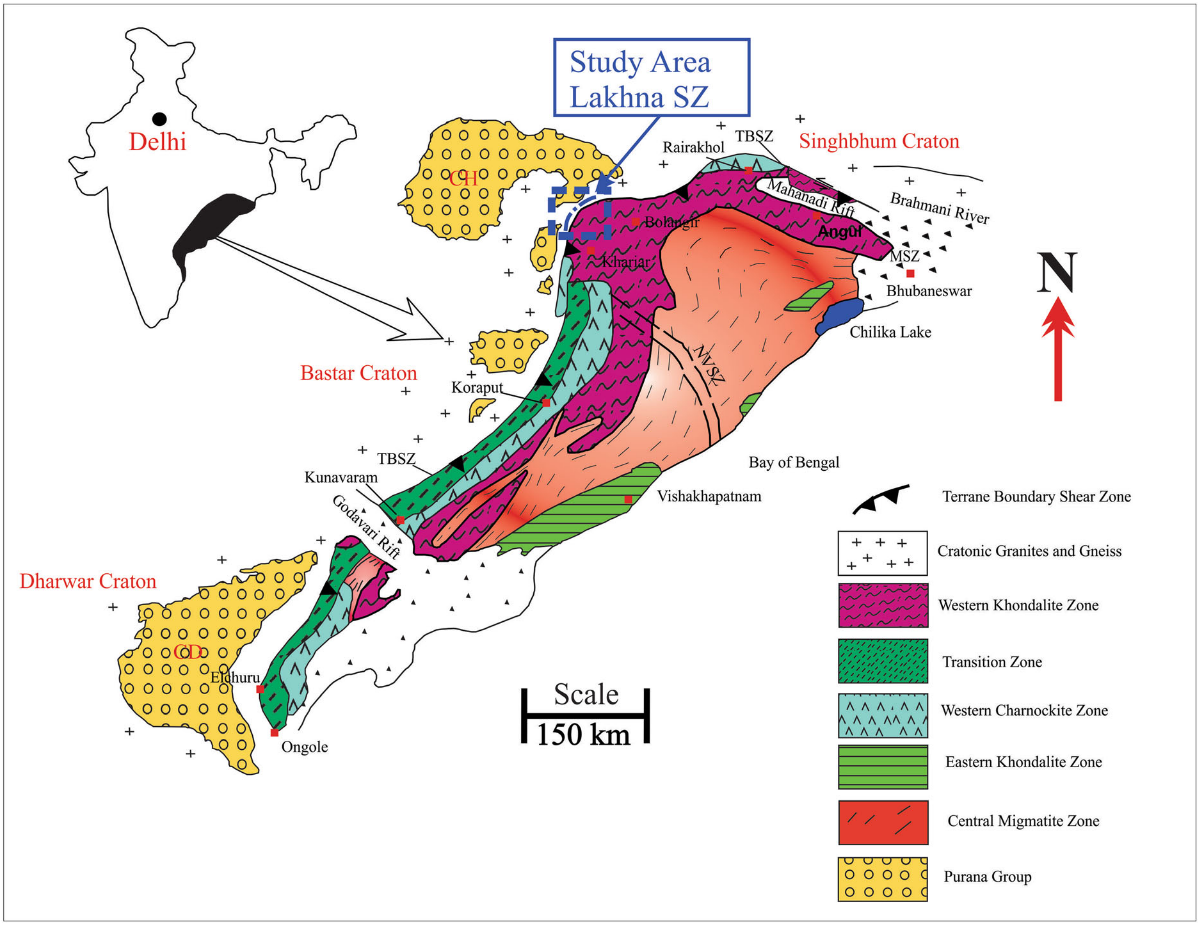


Figure 1. Longitudinal subdivisions of the EGMB (Ramakrishnan *et al.* 1998). In the study area, the western transition and charnockite zones are slivered and western khondalite zone rests directly over the Bastar Craton. The Bastar Craton is overlain by Purana basin rocks namely, CH: Chhattisgarh, KH: Khariar, AM: Ampani, CD: Cuddapah.

charnockite zones have been tectonically slivered in Lakhna area (Biswal 1998; Biswal *et al.* 1998; Biswal and Sahoo 1998; Ramakrishnan *et al.* 1998; Nanda 2008) and therefore, the western khondalite zone overlies the Bastar Craton. Though transitional zone is not in true sense of the term, it represents a sheared and retrograded zone. A detailed structural and geochronological work of the Lakhna shear zone and the overlying EGMB has come out with an imbricate thrust-belt structure in the EGMB, consisting of Sinapalli nappe, Lathore nappe and Turekela nappe (Biswal *et al.* 2007). The Sinapalli nappe consists of mafic granulites, Lathore nappe consisted of charnockites and Turekela nappe consisted of khondalites. The Lathore nappe directly overlies the Lakhna shear zone and is characterized by charnockites having alternate dark and light gneissic layers of mafic minerals as garnet–hypersthene–biotite and felsic minerals like quartz–K-feldspar–plagioclase feldspar. The gneissosity is axial planar to $F_1$ isoclinal to reclined fold which was syntectonic with the granulite facies metamorphism. Subsequent folding gave rise to open-to-tight $F_2$ folds and produced sheath folding during thrusting (Biswal *et al.* 1998). The sheath folds are folded by NW–SE $F_3$ folds. Besides these folding, a replication of a large scale fault-bend fold was deduced over a lateral ramp on the TBSZ (Biswal and Sinha 2003). The earlier structural fabrics have been reoriented to the shear direction (Gupta *et al.* 2000). Contrast to the mobile belt, the Bastar Craton is dominated by ca. 2.5 Ga granite, which does not show any sign of deformation except along the shear zone. The granite is coarse grained and consists of quartz, K-feldspar and biotite. Several N–S trending ca. 1.4 Ga old dolerite, rhyolite and trachyte dykes intrude the granite, which are also undeformed. The NNE trending 2 km wide Lakhna shear zone is developed dominantly on this ca. 2.5 Ga old granitic parent rock. The charnockites of the EGMB is affected by shearing. The width of such shear zone within the

EGMB is very thin. The temperature variation across the shear zone ranges from 700 to 550°C that has been explained due to over-thrusting of high temperature granulite rocks of the EGMB over cold Bastar Craton (Bhadra *et al.* 2004). At several places, the shear zone is intruded by alkaline rocks namely Koraput (Nanda *et al.* 2009), Khariar (Lakhna, Biswal *et al.* 2007) and at Rairakhol (figure 1). These alkaline rocks produce ages from 1.2 to 0.5 Ga suggesting different period of reactivation. The platform sequence namely the Khariar and the Ampani have been deformed by such thrusting (Ratre *et al.* 2010).

## 3. Methodology

### 3.1 *Microscopic study*

Fieldwork was carried out to update the existing geological map of the Lakhna shear zone (figure 2, Biswal *et al.* 2002). Petrofabric study and strain analyses of the shear zones were carried out on 15 oriented samples collected at regular intervals (approximately 200 m) over several profile lines (figure 2). The collected samples are cut into thin-sections perpendicular to foliation, one set is oriented parallel to the stretching lineation (XZ section) and the other perpendicular to stretching

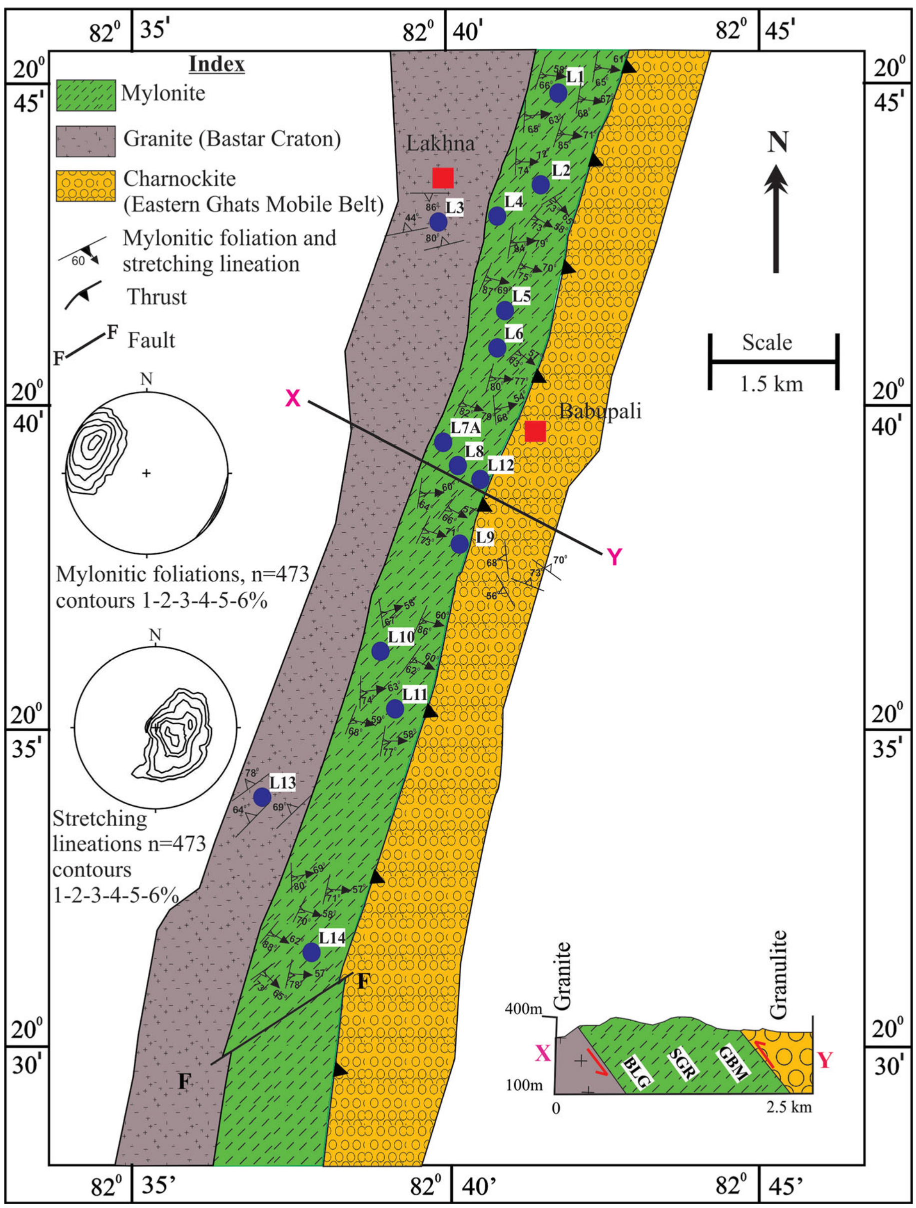


Figure 2. Geological map of the Lakhna shear zone. Stereoplots show mylonitic foliation and stretching lineations. Structural cross section along X–Y and have plotted BLG, SGR and GBM recrystallization along the section from craton to mobile belt boundary.

lineation (YZ section). The XZ sections are used for vorticity analysis and microstructure studies. The YZ sections are used for the identification of mineral assemblages of the different lithologies. A detailed description of the mineral content and microstructures was done using a Leitz optical microscope. The magnification of the lenses ranged from 1.2 to 20. The sections which contain 80–90% by volume of quartz grains were chosen for the study. This would avoid pinning of quartz grains by biotite.

### 3.2 *Piezometric calculation*

The quartz grains are significantly sensitive to the dislocation creep deformation in the mid to lower crust (e.g., Dunlap *et al.* 1997; Stipp *et al.* 2002). They uniquely respond to the differential stress produced during the ductile thrusting. A specific type of dislocation creep microstructure deformation is associated with certain differential stress. The material flow under such condition influences the size of the quartz grain at different stages of dynamic recrystallization. Hence, a good correlation can be established between differential flow stress and mean grain size. The equation used for piezometer calculation is as follows:

$$\sigma = B\, d^{-p}, \tag{1}$$

where $\sigma$ is the differential flow stress, $d$ is the mean grain size (in μm). $B$ (668.95) and $p$ (0.7936) depend upon the specific material properties and are derived experimentally (Stipp and Tullis 2003). Equation (1) is independent to temperature, water content and alpha–beta transition in quartz (Twiss 1977; Stipp *et al.* 2006; Twiss and Moores 2007). We have considered the grain size < 120 μm for the piezometric calculation, since a certain minimum lower limit of stress has no significant effect on the larger porphyroclast (e.g., >120 μm) (Stipp *et al.* 2010). The size of an irregular clast is considered as the diameter of the equivalent area of the circle of the same clast under a sectional plane. The standard plot of grain size *vs.* stress data of the quartz grain is used to decipher the deformation mechanism across the Lakhna shear zone. The temperature *vs.* stress graph (Platt and Behr 2011) helps to recognize the stress driven recrystallization process that developed the formation of new grains and the growth of grain during ductile shearing. The ACF (auto correction function) (Stipp *et al.* 2002) is not applied as the size measurement has been done manually by drawing the margin of the individual grain in the unprocessed image. Further, 3D correction (Boutonnet *et al.* 2013) is not done as the entire exercise is a 2D analysis of the grain size on XZ section.

### 3.3 *Vorticity estimation*

Shear zones generally undergo simple shear deformation. However, a different proportion of pure shear component exists with simple shear (Passchier and Trouw 2005). The relative proportion of simple shear and pure shear is not uniform across the shear zone. The mean kinematic vorticity number ($W_m$) is a measure of the relative proportion of simple to pure shear. The $W_m$ value is '1' for simple shear and '0' for pure shear. However, the $W_m$ value varies from 1 to 0 depending on the proportion of simple and pure shear during deformation. The $W_m$ can be measured using the aspect ratio and the orientation of the porphyroclasts as well as recrystallized grains (Ghosh and Ramberg 1976; Passchier 1987). Here, we have estimated the $W_m$ values using recrystallized quartz grains. We have used $R_s/\theta$ method, where $R_s$ represents the strain ratio on the XZ plane and can be obtained using $R_f/\Phi$ method ($R_f$: aspect ratio of clast and $\Phi$: orientation of long axis of porphyroclasts with the shear plane; Ramsay 1967; Lisle 1985) and $\theta$ is the angle between S-plane with the C-fabric. All angles and aspect ratio of the porphyroclasts are measured using imageJ software. The $W_m$ value is calculated as follows (Xypolias 2010):

$$W_m = \cos\left[\tan^{-1}\left(\frac{1 - R_s \tan^2\theta}{(1 + R_s)\tan\theta}\right)\right]. \tag{2}$$

A minimum of 100 grains (e.g., $n$ = 100–150; table 2) are used for samples L1, L6, L7A and L8A, whereas less than 100 grains (e.g., $n$ = 46–87) are used for samples L9 and L12. This decrease in numbers ($n$) is obvious with the growth of recrystallized grain size at the expense of the smaller grains towards the eastern part of the shear zone.

## 4. Results and discussion

### 4.1 *Field and microstructures of the Lakhna shear zone*

The Lakhna shear zone is dominated by quartzofeldspathic mylonite and protomylonite that are

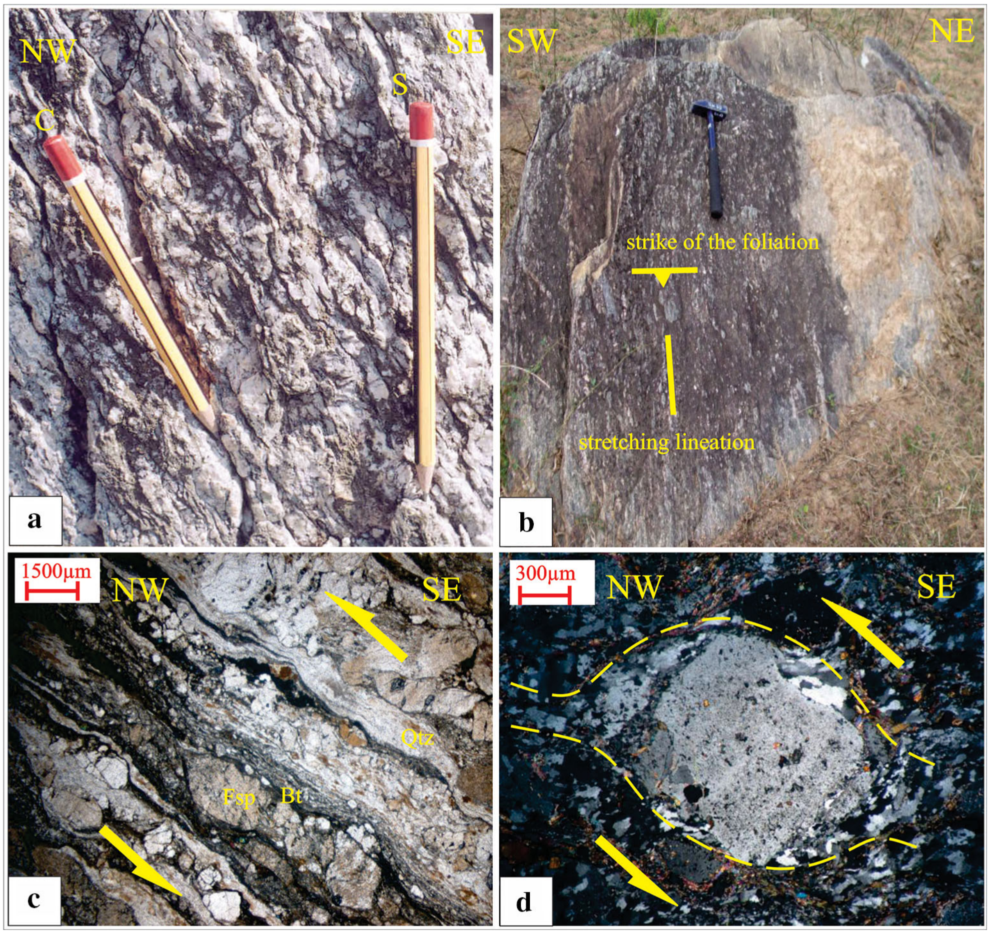


Figure 3. (**a**) Field photograph of granite mylonite showing foliation, feldspar porphyroclasts and S-C fabric suggesting NW vergence shear, vertical section, pencil (right) length 14 cm, (**b**) down-dip stretching lineations, defined by stretched quartz grains, vertical section, hammer is 12 inch, (**c**) mylonitic foliation defined by quartz ribbons (Qtz), biotitic rich layers (Bt) and feldspar layers (Fsp), and (**d**) sigma type feldspar porphyroclasts showing NW vergence.

characterized by well-defined mylonite foliation with a large number of porphyroclasts (figure 3a), down the dip stretching lineation (figure 3b) and the S-C fabric in the outcrop (figure 3a). The lineations are defined by stretching of quartz grains and biotite. The S-C fabric and rotated porphyroclasts indicate top-to-NW vergence thrust kinematics. Stereoplots of mylonitic foliations show concentration in NW quadrant and lineations in the SE quadrant consistent with thrust slip kinematics (figure 2, stereoplots). The photomicrograph shows mylonitic banding, characterized by quartz ribbons, biotite-rich layers and feldspar porphyroclasts-rich layers (figure 3c). The K-feldspar porphyroclasts stand out as a rigid grain within the matrix of phyllosilicate minerals of biotite with well-developed core mantle structure (figure 3d). There is no dynamic recrystallization associated with feldspar. The asymmetrical wings of the $\sigma$-type porphyroclasts specify top-to-NW vergence of shear. Quartz ribbons contain dynamically recrystallized quartz grains. During dynamic recrystallization, the grain boundary moves towards the higher strain zone, as a result new small bulging grains are formed surrounding the larger grain (figure 4a). This is a characteristic phenomenon of low temperature dynamic recrystallization deformation of grain boundary bulging (BLG). This bulging (BLG) mechanism of the grain boundary is obtained in samples close to the western boundary of the shear zone near the Bastar Craton (Sample L7A, figure 4a). The central part of the shear zone shows subgrain rotation (SGR), where quartz grains are recrystallized surrounding the porphyroclasts (Sample L1, L6, L8A; figure 4b). The deformation of the shear zone is gradually preceded with increasing recrystallized grain size and deformation temperature from west

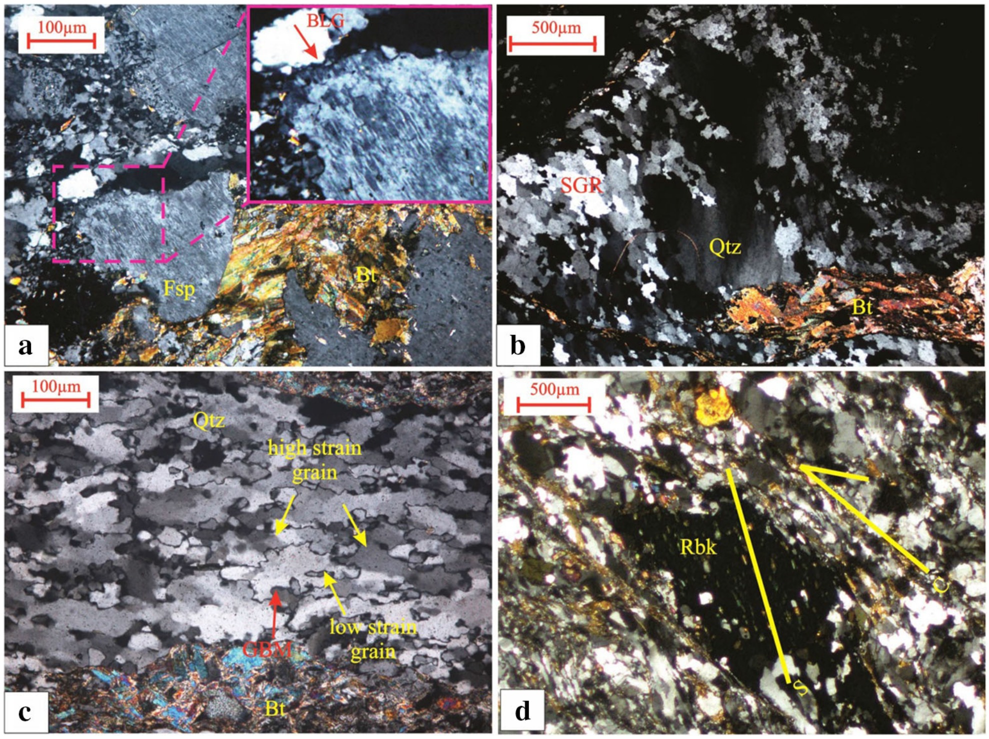


Figure 4. Photomicrograph of granite mylonite. (**a**) BLG recrystallization, (**b**) SGR, (**c**) GBM recrystallization of quartz grains, and **(d)** S-C fabric. S defines the maximum stretching direction.

to east (figure 5b). These recrystallized grains are oriented themselves parallel to the stretching direction of the strain ellipsoid defining S-C fabric in the rock (figure 4d). Places close to the EGMB boundary, produces a high strain rate of deformation that helps to migrate grain boundary into neighbouring minerals. The highly serrated grain boundary features reflect a high temperature deformation phenomenon with readily diffusion of elements from surrounding minerals which is commonly known as grain boundary migration (GBM) (Sample L9, L12; figure 4c). These recrystallized grains are strain free with no undulose extinction in it. In few instances, transgranular fractures are developed in the GBM grains during the strain hardening (Vollbrecht *et al.* 1999; Ghosh *et al.* 2016). From the dynamic recrystallization study of quartz grains, majority of the clasts are found in the SGR group where BLG occurs towards west and GBM towards the eastern part of the Lakhna shear zone (table 1; figure 2, profile section).

### 4.2 *Temperature of deformation*

Mylonites of the Lakhna shear zone contain biotite–quartz-rich assemblage suggesting green schist facies of metamorphism during shearing. Previously, it was reported that amphiboles (riebeckite) appear in the eastern part close to EGMB (Sinha 2004). Figure 5 shows grain size *vs.* frequency distribution. The sample L7A shows average grain size to be 26.6 μm for BLG, samples L1, L6 and L8A show a mean size variation from 60.40 to 60.92 μm for SGR recrystallization process and the samples L9 and L12 show a mean size from 87.21 to 99.45 μm for GBM recrystallization process (table 1). Figure 6 shows the grain size *vs.* temperature graph suggesting a transition from BLG (L7A) to SGR (sample L1, L6 and L8A) and GBM (sample L9 and L12). It is observed that with increase in temperature the grain size also increases from west to east (figure 5b). The temperature of recrystallization is estimated to be 380–420°C for BLG, 420–520°C for SGR and 550–560°C for GBM. Thus, temperature increases from 380 to 560°C from the Bastar Craton margin to the Eastern Ghats margin. The biotite rich mineral assemblage (figure 4a) at western part and gradually converting to riebeckite (figure 4d) at the eastern part also suggest the increasing temperature from west to east. So, thrusting probably took place when the EGMB was still hot and the craton was cool. The higher temperature of the EGMB

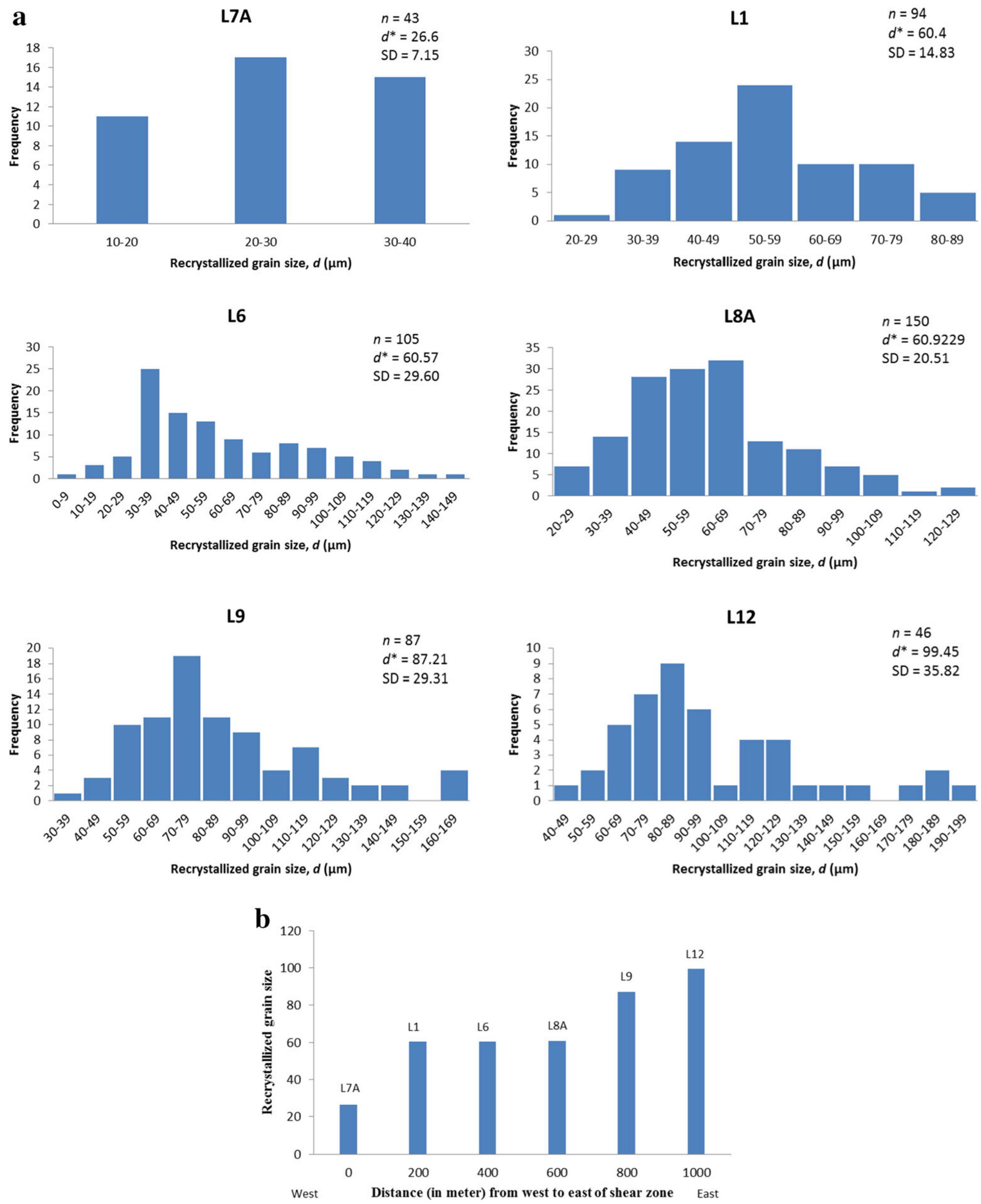


Figure 5. (**a**) Grain size *vs.* frequency plot of recrystallized quartz from the Lakhna shear zone (see figure 2 for locations). The mean size ($d^*$) varies from 26.6 to 99.45 μm with the standard deviation (SD) and '$n$' denotes the number of grains measured for each samples, and (**b**) graph indicates the average recrystallized grain size increases from west to east across the Lakhna shear zone.

favoured high temperature deformation in the east. The range of temperature deduced from grain size analysis is consistent with the result by Bhadra *et al.* (2004) who reported a temperature variation from 550° to 700°C across the TBSZ and based on their result they postulated that the EGMB was thrusted as a hot slab over cold Bastar Craton.

### 4.3 *Differential stress*

Here, we have plotted the graph between mean grain size and the differential flow stress to decipher the grain size evolution with creep dynamic recrystallization process across the Lakhna shear zone (figure 7; Platt and Behr 2011). The $D_{\mathrm{min}}$ line in the graph is defined by the minimum size of the nucleation that can be formed by the bulging process. The area above the $D_{\mathrm{min}}$ line indicates that grain growth is driven by strain energy ($\rho$GBM) (Derby 1992) rather than surface energy ($\gamma$GBM) (Platt and Behr 2011). From the analysis, we found that the samples fall closely above the $D_{\mathrm{min}}$ line maintaining a similar slope as the $D_{\mathrm{min}}$ line. In other words, the production of

Table 1. *The data represents different temperature associated with the dynamic recrystallization of quartz grain with evolving grain size and stress condition across the Lakhna shear zone.*

| Sample no. | Recrystallization mechanism | Deformation temperature (°C) | Grain size ($d$) (μm) | | Differential stress ($\sigma$) (MPa) | | |
|---|---|---|---|---|---|---|---|
| | | | Average | SD | Minimum | Average | Maximum |
| L7A | BLG | 380–420 | 26.6 | 7.15 | 37.8597 | 49.5002 | 87.9623 |
| L1 | SGR | 430–490 | 60.40 | 14.83 | 18.9354 | 25.8203 | 45.5242 |
| L6 | SGR | 430–490 | 60.57 | 29.60 | 12.9125 | 25.7623 | 89.5957 |
| L8A | SGR | 430–520 | 60.92 | 20.51 | 14.1681 | 25.6443 | 53.121 |
| L9 | GBM | 550–560 | 87.21 | 29.31 | 11.4389 | 19.2899 | 40.7664 |
| L12 | GBM | 550–560 | 99.45 | 35.82 | 10.1042 | 17.3817 | 30.9862 |

Table 2. *Mean kinematic vorticity ($W_m$) is determined using recrystallized quartz grains of mylonitic samples (figure 2).*

| Sample no. | S-C angle ($\theta$) | Strain ratio ($R_s$) | Vorticity ($W_m$) | Simple shear (%) | No. of grains ($n$) | Dominant shear |
|---|---|---|---|---|---|---|
| L1 | 32 ± 6 | 2.197 ≈ 2.2 | 0.98 | 88 | 118 | Simple shear |
| L6 | 32 ± 4 | 2.023 ≈ 2.0 | 0.98 | 88 | 105 | Simple shear |
| L7A | 33 ± 9 | 2.576 ≈ 2.6 | 0.98 | 88 | 100 | Simple shear |
| L8A | 32 ± 9 | 2.012 ≈ 2.0 | 0.98 | 88 | 150 | Simple shear |
| L9 | 35 ± 5 | 2.155 ≈ 2.1 | 0.99 | 92 | 87 | Simple shear |
| L12 | 33 ± 5 | 2.256 ≈ 2.3 | 0.99 | 92 | 46 | Simple shear |

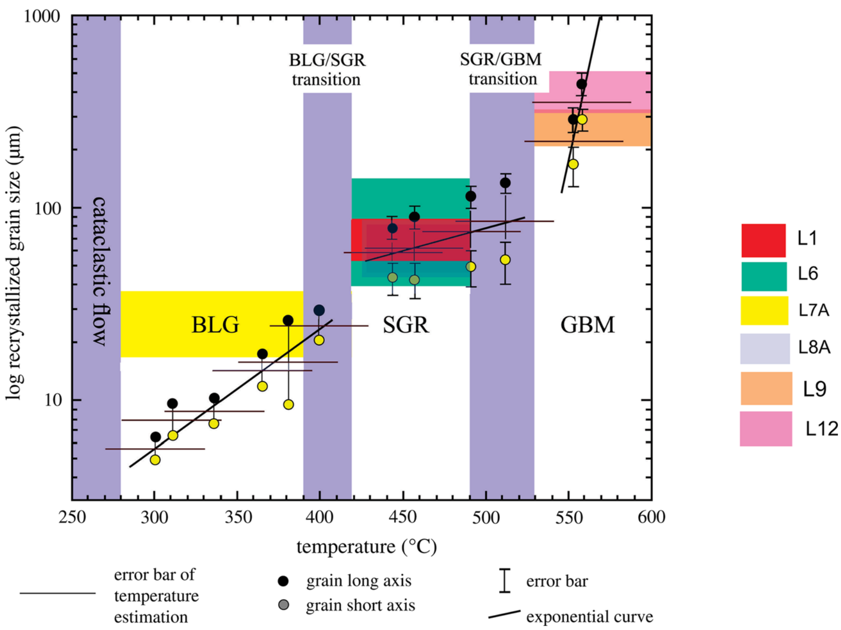


Figure 6. The grain size *vs.* $T$ plot (after Stipp *et al.* 2002) indicating temperature at different mode of recrystallization of quartz grains in the Lakhna shear zone.

nucleation is governed by the BLG mechanism. The deformation process has predominantly shifted from creep dominated by grain boundary sliding (low $T$) to climb-dislocation creep (high $T$). Since most of the samples are present in the climb assisted dislocations creep, only one sample is in the DRX creep field (figure 7a). The deformation mechanism proceeds from high differential stress and low temperature to low differential stress and high temperature condition from west to east (figure 7b). Further, the strain rate also increases from west ($10^{-14}$ $s^{-1}$) to east ($10^{-12}$ $s^{-1}$) (figure 7b). In this process, the grain growth occurs by moving grain boundary convex outward into the

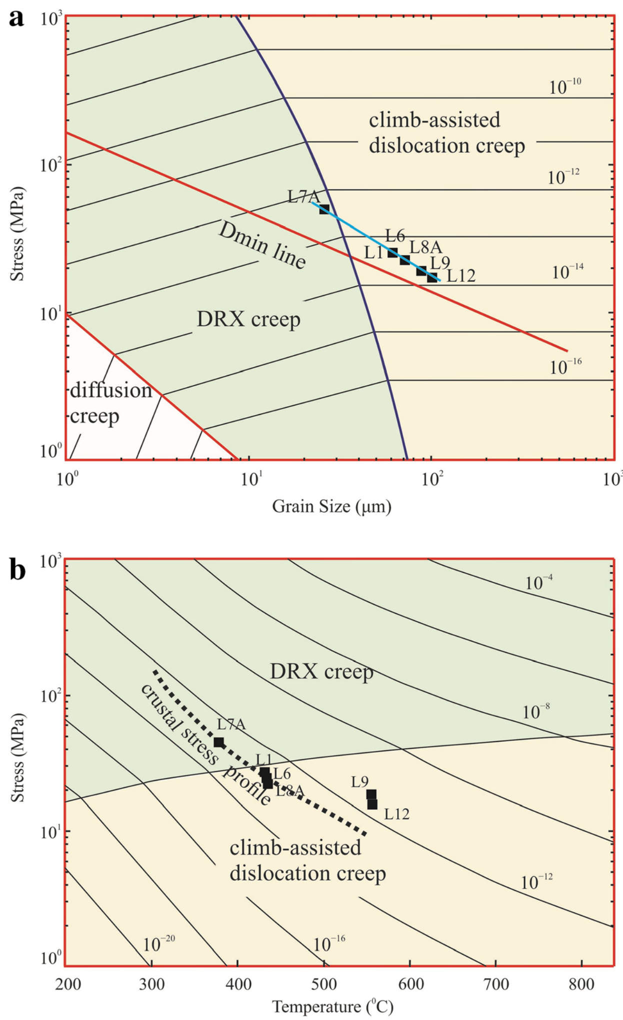


Figure 7. (**a**) Stress *vs.* grain size graph for the deformation creep mechanism of quartz (Platt and Behr 2011). The $D_{\min}$ line indicates the minimum size of the nucleation that can be produced by BLG mechanism at a certain stress condition. The best fit line of the data points falls above the $D_{\min}$ line shows a $\rho$GBM dominant field of grain growth. Most of the samples show a SGR recrystallization deformation with climb assisted dislocation creep, and (**b**) stress *vs.* temperature graph indicating stress value drops, while strain increases with increase in temperature.

direction of greater dislocation density grain (figure 4c, the red arrow indicates convex outward growth).

### 4.4 *Mean kinematic vorticity*

The vorticity ($W_m$) calculation using equation (2) shows 0.98 and 0.99 for the samples (table 2). Our results do not show much variation in vorticity across the Lakhna shear zone. All the points are clustered around the $W_m = 1$ line (figure 8) within a maximum error of S-C angle $\theta = \pm 9$ (table 2).

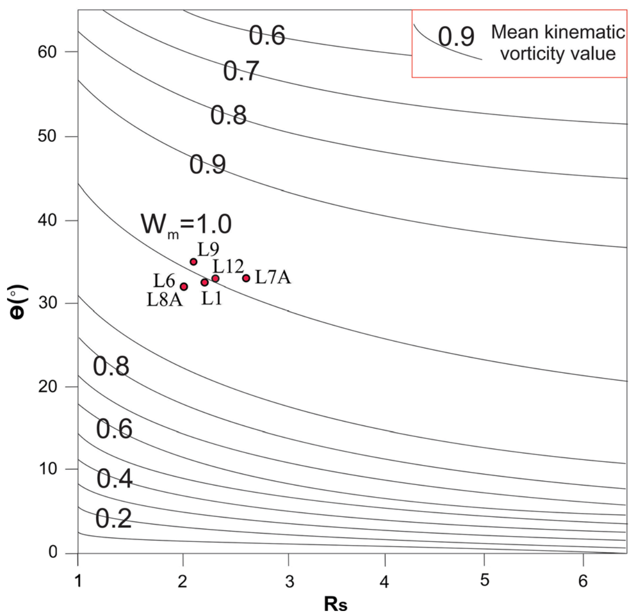


Figure 8. The graph shows the mean kinematic vorticity ($W_m$) analysis of recrystallized quartz grain. All points are clustered near $W_m = 1$ contour line indicating a dominant simple shear phenomenon (after Tikoff and Fossen 1995).

The analysis indicates that the deformation along the Lakhna shear zone is dominated by simple shear with a little pure shear contribution. Hence, the mechanism of recrystallization has very less effect on the nature of strain during the thrust kinematic process in the Lakhna shear zone. Deformation by simple shear suggests that the compressive stress was at right angle to strike of the thrust plane and there was no oblique slip component (Jones *et al.* 2004).

## 5. Conclusion

The Lakhna shear zone indicates a simple shear deformation with thrust kinematics. The EGMB has been thrusted over the Bastar Craton. Previously, the age of thrusting was determined to be ca. 0.5 Ga. The Lakhna shear zone has developed primarily on granites of the Bastar Craton and the mylonites in the shear zone are quartzofeldspathic in composition. Petrographic study of the mylonites and grain size measurement of quartz grains in mylonites reveal that the shear zone has undergone BLG at the western margin to SGR in the central part and GBM at the eastern margin. The temperature of deformation has evolved through 360–380°C for BLG, 420–490°C for SGR and 530–560°C for GBM crystallization suggesting an increase in temperature of deformation from west to east. The higher temperature of deformation towards the hanging wall of the EGMB margin suggests that the EGMB granulitic block was thrusted as a hot slab over cold Bastar Craton. Quartz grain size increases with the rise in temperature. The grain size evolution was driven by strain energy rather than surface energy. The mean kinematic vorticity ($W_m$) estimation suggests that the Lakhna shear zone was dominated by simple shear deformation. The presence of a few pure shear indicates that the compressive stress during thrusting was right angle to the strike of the thrust plane. Hence, the juxtaposition of the EGMB with the Bastar Craton during Cambrian–Neoproterozoic period was manifested in form of a simple shear dominating thrust in the NW margin of the mobile belt and the thrust displays a variation in temperature and dynamics of recrystallization from craton to mobile belt.

## Acknowledgements

The authors acknowledge the Central University of Kerala, India for allowing field work in and around Lakhna, Odisha and the Indian Institute of Technology Bombay (IITB) for providing lab facilities for petrofabric analysis of thin sections of mylonite samples. We also thank Associate Editor Prof. Saibal Gupta for handling this manuscript and other anonymous reviewer.

## References

Aftalion M, Bowes D R, Dash B and Fallick A E 2000 Late Pan-African thermal history in the Eastern Ghats terrane, India, from U–Pb and K–Ar isotopic study of the Mid-Proterozoic Khariar alkali syenite, Orissa; *Geol. Surv. India* **57** 26–32.

Boutonnet E, Leloup P H, Sassier C, Gardien V and Ricard Y 2013 Ductile strain rate measurements document long-term strain localization in the continental crust; *Geology* **41(8)** 819–822.

Bhadra S, Gupta S and Banerjee M 2004 Structural evolution across the Eastern Ghats Mobile Belt-Bastar craton boundary, India: Hot over cold thrusting in an ancient collision zone; *J. Struct. Geol.* **26(2)** 233–245.

Biswal T K 1998 The lithotectonic setting of the Eastern Ghat Mobile Belt and adjoining craton in western Orissa, India: An example of Mesoproterozoic Fold-Thrust Belt; *Gondwana Res.* **1** 410–412.

Biswal T K and Sahoo D 1998 IRS-1C digital data interpretation of lithotectonic setting in northwestern part of the Eastern Ghats Mobile Belt, Orissa; *Curr. Sci.* **75(8)** 846–850.

Biswal T K, Sajeevan G and Nayak B P 1998 Deformational history of Eastern Ghats Mobile Belt around Lathore, Balangir district, Orissa; *J. Geol. Soc. India* **51** 219–225.

Biswal T K 2000 Fold-thrust belt geometry of the Eastern Ghats Mobile Belt, a structural study from its western margin, Orissa, India; *J. African Earth Sci.* **31(1)** 25–33.

Biswal T K, Jena S K, Datta S, Das R and Khan K 2000 Deformation of terrane boundary shear zone (Lakhna shear zone) between Eastern Ghats Mobile Belt and Bastar craton in Balangir and Kalahandi districts, Orissa; *J. Geol. Soc. India* **55(4)** 367–380.

Biswal T K, Biswal B, Mitra S and Moulik M R 2002 Deformation pattern of the NW terrane boundary of the Eastern Ghats Mobile Belt, India: A tectonic model and correlation with Antarctica; *Gondwana Res.* **51** 45–52.

Biswal T K and Seward D 2003 Tectonic implication of the apatite fission-track analysis of the mylonites from the terrane boundary shear zone of the eastern Ghats mobile belt around Lakhna, Orissa; *Gondwana Res.* **6(2)** 321–325.

Biswal T K and Sinha S 2003 Deformation history of the NW salient of the Eastern Ghats Mobile Belt, India; *J. Asian Earth Sci.* **22** 157–169.

Biswal T K, Ahuja H and Sahu H S 2004 Emplacement kinematics of nepheline syenites from the Terrane Boundary Shear Zone of the Eastern Ghats Mobile Belt, west of Khariar, NW Orissa: Evidence from meso-and microstructures; *J. Earth Syst. Sci.* **113(4)** 785–793.

Biswal T K, De Waele B and Ahuja H 2007 Timing and dynamics of the juxtaposition of the Eastern Ghats Mobile Belt against the Bhandara Craton, India: A structural and zircon U–Pb SHRIMP study of the fold-thrust belt and associated nepheline syenite plutons; *Tectonics* **26(4)** 1–21.

Crookshank H 1963 Geology of southern Bastar and Jeypore from the Bailadila range to the Eastern Ghats; *Geol. Surv. India Memoir* **87** 1–150.

Derby B 1992 Dynamic recrystallization: The steady state grain size; *Scr. Metall. Mater.* **27** 1581–1586.

Dunlap W J, Hirth G and Teyssier C 1997 Thermomechanical evolution of a ductile duplex; *Tectonics* **16** 983–1000.

Fermor L L 1936 An attempt at the correlation of the ancient schistose formations of peninsular India; *Geol. Surv. India Memoir* **70** 1–324.

Fossen H and Tikoff B 1993 The deformation matrix for simultaneous simple shearing, pure shearing and volume change, and its application to transpression-transtension tectonics; *J. Struct. Geol.* **15(3–5)** 413–422.

Ghosh S K and Ramberg H 1976 Reorientation of inclusions by combination of pure shear and simple shear; *Tectonophys.* **34(1)** 1–70.

Ghosh S, Bose S, Mandal N and Dasgupta S 2016 Dynamic recrystallization mechanisms and their transition in the Daling Thrust (DT) zone, Darjeeling–Sikkim Himalaya; *Tectonophys.* **674** 166–181.

Grew E S and Manton W I 1986 A new correlation of sapphirine granulites in the Indo-Antarctic metamorphic terrain: Late Proterozoic dates from the Eastern Ghats province of India; *Precamb. Res.* **33(1–3)** 123–137.

Gupta S, Bhattacharya A, Raith M and Nanda J K 2000 Contrasting pressure–temperature–deformation history across a vestigial craton–mobile belt boundary: The western margin of the Eastern Ghats Belt at Deobhog, India; *J. Metamorph. Geol.* **18(6)** 683–697.

Jones R R, Holdsworth R E, Clegg P, McCaffrey K and Tavarnelli E 2004 Inclined transpression; *J. Struct. Geol.* **26(8)** 1531–1548.

Lal R K, Ackermand D and Upadhyay H 1987 PTX relationships deduced from corona textures in sapphirine-spinel-quartz assemblages from Paderu, southern India; *J. Petrol.* **28(6)** 1139–1168.

Lisle R J 1985 The use of the orientation tensor for the description and statistical testing of fabrics; *J. Struct. Geol.* **7(1)** 115–117.

Leelanandam C 1990 The anorthosite complexes and Proterozoic mobile belt of peninsular India: A review; *Dev. Precamb. Geol.* **8** 409–435.

Leelanandam C 1993 Alkaline magmatism in the Eastern Ghat Belt – A critique; *J. Geol. Soc. India* **42(5)** 435–447.

Nanda J K 2008 Tectonic framework of Eastern Ghats mobile belt: An overview; *Geol. Soc. India Memoir* **74** 63–87.

Nanda J, Gupta S and Mamtani M A 2009 Analysis of deformation fabric in an Alkaline Complex (Koraput): Implications for time relationship between emplacement, fabric development and regional tectonics; *J. Geol. Soc. India* **74(1)** 78–94.

Nanda J K and Pati U C 1989 Field relation and petrochemistry of the Granulites and associated rocks in the Ganjam–Koraput sector of the Eastern Ghats Belts; *Ind. Mineral.* **43** 247–264.

Nanda J K, Rath S C and Behera S N 1998 Alkaline and ultramafic magmatism in the contact zone between high and low grade terrains: Example from NW Orissa, India; In: Precambrian Crust in Eastern and Central India; *Geol. Surv. India Publ.,* Bhubaneswar, India, pp. 122–130.

Neogi S and Das N 1998 Lithotectonic domains and metamorphic history of the boundary zone of the Eastern Ghats orogen and Bastar craton. Deobhog area, Madhya Pradesh and its implication; *Precambrian Crust Eastern and Central India,* pp. 180–204.

Passchier C W 1987 Stable positions of rigid objects in noncoaxial flow – A study in vorticity analysis; *J. Struct. Geol.* **9(5–6)** 679–690.

Passchier C W and Urai J L 1988 Vorticity and strain analysis using Mohr diagrams; *J. Struct. Geol.* **10(7)** 755–763.

Passchier C W and Trouw R A J 2005 *Microtectonics*; 2nd edn, Springer, Berlin.

Platt J P and Behr W M 2011 Grain size evolution in ductile shear zones: Implications for strain localization and the strength of the lithosphere; *J. Struct. Geol.* **33** 537–550.

Ramsay J G 1967 *Folding and fracturing of rocks*; McGraw-Hill, New York, pp. 103–109.

Ramsay J G and Huber M I 1983 *The Techniques of Modern Structural Geology, Strain Analysis*; Academic Press, London.

Ramsay J G and Huber M I 1987 *The Techniques of Modern Structural Geology*; Academic press, London.

Ramakrishnan M 1990 Crustal development in southern Bastar, central India craton; *Geol. Surv. India Spec. Publ.* **28** 44–66.

Ramakrishnan M, Nanda J K and Augustine P F 1998 Geological evolution of the Proterozoic Eastern Ghats mobile belt; *Geol. Surv. India Spec. Publ.* **44** 1–21.

Ratre K, De Waele B, Biswal T K and Sinha S 2010 SHRIMP geochronology for the 1450 Ma Lakhna dyke swarm: Its implication for the presence of Eoarchaean crust in the Bastar Craton and 1450–517 Ma depositional age for Purana basin (Khariar), Eastern Indian Peninsula; *J. Asian Earth Sci.* **39(6)** 565–577.

Sarkar G, Corfu F, Paul D K, McNaughton N J, Gupta S N and Bishui P K 1993 Early Archean crust in Bastar Craton, Central India – A geochemical and isotopic study; *Precamb. Res.* **62(1–2)** 127–137.

Sarkar A and Paul D K 1998 Geochronology of the Eastern Ghats Precambrian mobile belt – A review; *Geol. Surv. India Spec. Publ.* **44** 51–86.

Simpson C and De Paor D G 1993 Strain and kinematic analysis in general shear zones; *J. Struct. Geol.* **15(1)** 1–20.

Sinha S 2004 Strain analysis of the Terrane Boundary Shear Zone developed between the Bastar Craton and the Eastern Ghats Mobile Belt, around Lakhna, Nawapara district, Orissa, India; Unpubl. Ph.D. thesis, IIT-Bombay, India.

Sinha S, Alsop G I and Biswal T K 2010 The evolution and significance of microfracturing within feldspars in low-grade granitic mylonites: A case study from the Eastern Ghats Mobile Belt, India; *J. Struct. Geol.* **32(10)** 1417–1429.

Stipp M, Stünitz H, Heilbronner R and Schmid S M 2002 Dynamic recrystallization of quartz: Correlation between natural and experimental conditions; *Geol. Soc. London, Spec. Publ.* **200(1)** 171–190.

Stipp M and Tullis J 2003 The recrystallized grain size piezometer for quartz; *Geophys. Res. Lett.* **30** 2088.

Stipp M, Tullis J and Behrens H 2006 Effect of water on the dislocation creep microstructure and flow stress of quartz and implications for the recrystallized grain size piezometer; *J. Geophys. Res.* **111** B04201.

Stipp M, Tullis J, Scherwath M and Behrmann J H 2010 A new perspective on paleopiezometry: Dynamically recrystallized grain size distributions indicate mechanism changes; *Geology* **38** 759–762, http://dx.doi.org/10.1130/G31162.1.

Tikoff B and Fossen H 1995 The limitations of three-dimensional kinematic vorticity analysis; *J. Struct. Geol.* **17(12)** 1771–1784.

Twiss R J 1977 Theory and applicability of a recrystallized grainsize paleopiezometer; *Pure Appl. Geophys.* **115** 227–244.

Twiss R J and Moores E M 2007 *Structural geology*; 2nd edn, W.H. Freeman and Company, New York.

Vollbrecht A, Stipp M and Olesen N Ø 1999 Crystallographic orientation of microcracks in quartz and inferred deformation processes: A study on gneisses from the German Continental Deep Drilling Project (KTB); *Tectonophys.* **303(1)** 279–297.

Wallis S R 1992 Vorticity analysis in a metachert from the Sanbagawa Belt, SW Japan; *J. Struct. Geol.* **14** 271–280.

Wallis S R, Platt J P and Knott S D 1993 Recognition of syn-convergence extension in accretionary wedges with examples from the Calabrian Arc and the Eastern Alps; *Am. J. Sci.* **293(5)** 463–494.

Wallis S 1995 Vorticity analysis and recognition of ductile extension in the Sanbagawa belt, SW Japan; *J. Struct. Geol.* **17(8)** 1077–1093.

Xypolias P and Kokkalas S 2006 Heterogeneous ductile deformation along a mid-crustal extruding shear zone: An example from the External Hellenides (Greece); *Geol. Soc. London, Spec. Publ.* **268** 497–516.

Xypolias P 2010 Vorticity analysis in shear zones: A review of methods and applications; *J. Struct. Geol.* **32(12)** 2072–2092.

Corresponding editor: Saibal Gupta